IEEE Access
Multidisciplinary | Rapid Review | Open Access Journal

Received 6 March 2024, accepted 24 May 2024, date of publication 28 May 2024, date of current version 6 June 2024.

Digital Object Identifier 10.1109/ACCESS.2024.3406550

RESEARCH ARTICLE

Robust Access Points Selection Strategies for Dynamic Indoor Localization

AQILAH BINTI MAZLAN AND YIN HOE NG
Faculty of Engineering, Multimedia University, Cyberjaya 63100, Malaysia
Corresponding author: Yin Hoe Ng (yhng@mmu.edu.my)

This work was supported by the Fundamental Research Grant Scheme (FRGS), Ministry of Higher Education Malaysia, under Grant FRGS/1/2023/ICT02/MMU/02/7.

ABSTRACT The proliferation of mobile devices has fueled the demand for indoor location-based services. Consequently, a plethora of techniques have emerged to facilitate object and device localization in indoor environments. Among these, fingerprint-based indoor localization systems, which leverage machine learning, stand out as a promising solution for providing accurate localization. Nonetheless, their performance is inherently reliant on the accuracy of the underlying database, and any changes in the indoor layout can significantly impact the wireless signals, subsequently affecting the localization accuracy. To circumvent this issue, this work proposes a novel access point (AP) selection framework to enhance the robustness of fingerprint-based indoor positioning systems in dynamic indoor environments. More specifically, a hybrid Wi-Fi and BLE fingerprint database is constructed by collecting received signal strength (RSS) from the pre-defined reference points (RPs). To ensure that the fingerprint database remains relevant over time, some RPs are designated as known points so that the system can periodically collect new RSS at the known points. Subsequently, the proposed scheme computes the differences between the RSS of the database and the updated RSS from the new layout to account for the changes occurred. The building-based, floor-based, and zone-based implementation modes determine which APs are reliable to be utilized during localization based on the RSS discrepancies observed in building, floor, and zone, respectively. Results demonstrate that the proposed building-based, floor-based, and zone-based AP selection schemes could achieve reduction in positioning error up to 28.86%, 33.53%, and 39.66%, respectively, compared to the baseline technique without AP selection schemes.

INDEX TERMS Indoor positioning system, fingerprinting, Wi-Fi, BLE, AP selection.

I. INTRODUCTION

The Internet of Things (IoT), which helps users access smart services in a smooth manner, have been heavily integrated into the industry across various fields. Consequently, the bulk of individuals rely extensively on IoT-enabled gadgets for their daily activities. Additionally, location-based services (LBS), applications that depend on the location of users to deliver information [1], are one of the most frequently used services by IoT devices. As a result, localization systems have continued to flourish during the recent decade as more discoveries on location-based technologies have become available. Currently, outdoor localization is achieved through the Global Positioning System (GPS). However, GPS is inapplicable in indoor areas due to non-line-of-sight limitations. Various technologies have been investigated for indoor positioning and mainstream wireless signals such as Wi-Fi [2], Ultra-wideband [3]. Bluetooth [4] and Zig Bee [5] are often used for this purpose. Fusion between two technologies, particularly the fusion of Wi-Fi and Bluetooth Low Energy (BLE) [6], have been explored in recent years for better performing indoor positioning system. A prevalent solution for the indoor localization problem is to estimate the position of users or devices through received signal strength (RSS) measurements [7] which are used alongside a position estimation algorithm, such as fingerprint-based algorithm and geometrical calculation. In a noise-free environment, the RSS can be modelled as follows [8]:

$$RSS = P - \beta - 10\alpha \log_{10} d, \tag{1}$$

The associate editor coordinating the review of this manuscript and approving it for publication was Jenny Mahoney.

where P represents the transmitted power, α represent the path loss exponent which falls linearly, and β is the constant that depends on the condition of the environment.

In real-world scenarios, indoor environments are dynamic and wireless signals are susceptible to noise contamination. These would complicate the usage of (1) for geometrical calculation in the localization process [9], [10]. Thus, fingerprint-based indoor positioning system is preferable in this scenario. Fingerprinting is a process that tags a specific location in the indoor environment to a unique identifier. This process is done in two stages which are the offline and online stage. In the offline stage, calibration is done by linking a location in the indoor space to a fingerprint, which is typically a feature or characteristic of the wireless signal. Then, the fingerprint is stored inside a database. The online stage consists of online query by the users, where the devices will receive real-time RSS. The position of the user will then be estimated via a matching algorithm that compares the real-time RSS to the ones stored in the database. The algorithms used to deduce the coordinate of user can be classified into two which are the deterministic algorithm [11] and the probabilistic algorithm [12]. Given a set of RSS input, a deterministic algorithm will output the same location each time the same input is fed into the system. As for the probabilistic algorithm, the distribution of fingerprint stored in the offline phase and the probability distribution will be analyzed. The real-time fingerprint is then compared with the distribution of fingerprint to infer the position of user or object [13].

As pointed out in [14], the real-world indoor environments experience both transient changes, which are dynamic alterations that occur briefly such as human mobility, and permanent changes like infrastructural changes. The fingerprinting approach is directly affected by the radio map constructed during the offline stage [15]. If the real-time RSS received by the user's device deviates from that of the previously recorded radio map, the system may fail to provide an accurate location. The disparities between the RSS readings from the same access points (APs) will subsequently affect the localization process.

In response to the challenges outlined above, this work introduces a novel AP selection framework to improve the robustness of fingerprint-based indoor positioning systems in dynamic indoor environments by excluding the APs that are adversely affected by the transient and permanent changes during the positioning phase. To the best of the authors' knowledge, there is no prior work on AP selection specifically addressing the enhancement of robustness of dynamic indoor positioning. The main contributions of our work are highlighted as follows:

1. A novel AP selection framework with three implementation modes is proposed to select reliable APs to be used during the fingerprint matching process. To determine the reliable APs, the system leverages a small percentage of the reference points (RPs) throughout the localization area, hereafter referred to as known points, to regularly collect updated RSS vectors so that the changes of RSS from a specific AP can be detected by the system. In the localization phase, only the APs with RSS deviations within the tolerance range will be employed.
2. An in-depth analysis is performed to assess the performances of the proposed AP selection scheme. The evaluation is conducted using a real-world hybrid Wi-Fi and BLE dataset that is collected in a multi-story building and the proposed AP selection scheme is benchmarked against the baseline positioning system without AP selection scheme to underscore the significance and advantages of utilizing the proposed techniques. In addition to key performance metrics such as the floor classification accuracy and average positioning error, the analysis also delves into the impact of layout change on the RSS variations from various APs and thoroughly examines the spatial distribution of positioning errors.
3. A comprehensive investigation is carried out to study the effects of various parameters associated with the proposed AP selection strategy. In particular, the effectiveness of the proposed AP selection framework under different implementation modes, number of known points and sub-regions are analyzed in detail to provide clear guidelines that ensure successful deployment of these techniques.

The rest of this paper is organized as follows. In Section II, an overview of the existing work is presented and discussed. A comprehensive explanation of the indoor positioning algorithm with the AP selection scheme under three implementation modes is described in Section III. Section IV elucidates the dataset and experimental environment. Section V provides a thorough investigation of the AP selection algorithms. Lastly, the paper concludes in Section VI.

II. RELATED WORKS

RADAR [16] has been acknowledged as the pioneering fingerprint-based indoor localization that was introduced back in 2000. It utilizes RSS measurements and a deterministic algorithm to estimate a user's indoor location accurately. Later, another commercial indoor localization system, HORUS [17], is presented in 2005 and it adopts a probabilistic strategy in which spatial and temporal RSS modellings are carried out. Since the introduction of RADAR and HORUS, numerous other fingerprint-based indoor positioning systems [18], [19], [20], [21] have been developed, each with its own improvements and innovations. The field of indoor localization has continued to evolve, and new technologies and techniques have emerged, making indoor positioning systems more accurate, efficient, and widely used for various indoor applications. Researchers have gone to great lengths to introduce countless positioning approaches, technologies, and algorithms to improve the performance of the indoor positioning technique, which is quantified using a

variety of criteria that account for the accuracy, robustness, efficiency, and user experience.

Diverse indoor positioning systems have been presented in the recent Indoor Positioning and Indoor Navigation (IPIN) competitions [22], [23], [24], encompassing smartphone-based positioning system and vision-based positioning systems. These systems leverage data from various sensors, such as Wi-Fi, BLE, accelerometer, magnetometer, barometer, and light sensor. The works in [22], [23], and [24] have also delved into various methodologies, including fingerprinting for location estimation, dead reckoning to obtain accurate trajectory estimation, and zero velocity update popularly used for foot-mounted inertial measurement unit-based localization. Among the works presented in [22], [23], and [24], only one from Track 5 of IPIN 2020 competition by the YONAYONA Team is relevant to AP selection. The team employs a Bluetooth low energy (BLE) beacon selection scheme to determine the absolute position by selecting three BLE beacons with high RSS. However, their primary objective is to ensure that the same number of beacons are utilized for positioning and it does not address the issue of environmental dynamics.

Several works have incorporated AP selection schemes [25] to their positioning system to select a subset of the most relevant and informative AP based on the optimization goals so that they can optimize the accuracy of the system [26], reduce computational complexity [27] and optimize the size of the database [28]. These works discovered that it is unnecessary to adopt all the available APs in localization but instead only utilize the reliable APs which have more contribution to the positioning process. Utilizing all the APs would only contribute in storage wastage. The authors in [29] define a Cramer-Rao lower bound to describe the localization error that generally occurs with commonly used Wi-Fi localization system. From there, they proposed a heuristic AP selection approach to bring down the size of the radio map to subsequently reduce the computational expense by only maintaining the AP with high contribution. The work in [27] proposed an AP selection standard that utilizes the maximum value of RSS and appearance ratio as indicators for the reliability of AP. Both a variance-based AP selection scheme and RP selection scheme are applied as an effort to efficiently shrink the fingerprint database while increasing the positioning accuracy of the fingerprint-based positioning system [28]. The RSS distribution of a specific AP can provide information about its spatial discrimination and, hence, AP with a variance lower than a particular value is filtered out. MAPS, a multiple access point selection-based indoor localization technique, was designed in [30]. The purpose of the AP selection algorithm is to simplify the computation of the system by selecting only a stable subset of AP, which reduces the fingerprint's dimension. In this method, the AP is first selected through a threshold where infrequent AP are eliminated. Following that, the set of APs is chosen using information gain, choosing those with a larger information gain and after location clustering is conducted, the AP is again reselected based on each cluster.

The distribution of RSS will be significantly impacted by changes to the indoor environment to a point that the existing radio map cannot provide an accurate representation of the current indoor environment. Thus, the impacts of environmental dynamics on indoor positioning systems are an essential aspect to investigate. Although environmental changes are introduced in the Track 7 of IPIN 2021 and IPIN 2022 [24] by moving mobile metallic object to test the robustness of the indoor positioning systems developed by the participating teams against environmental variations, the systems showcased in this track do not take into account AP selection. The positioning system in [31] make use of the hidden Markov Model algorithm to generate an adaptive radio map and the information gain AP selection technique is exploit by the system to increase the effectiveness of the proposed system. A localization system designed for dynamic indoor environment [32] makes use of expectation-maximization (EM) algorithm to filter out abnormal fingerprint brought on by the environment and a Bayesian-based simultaneous AP selection is proposed to select valuable APs for optimal matching in test phase. The AP selection strategy imposed on the positioning system in [33] takes the Gini impurity of an AP to evaluate its significance so that the system is able select good APs in dynamic environment. Instead of executing the AP selection strategy during the offline phase, the multi-objective-based self-adaptive AP selection algorithm [34] is performed at the online phase, with two major steps. In the first step, the learning algorithm automatically controls the number of the subset of APs and the loss rate threshold. Based on first step, mean-max-based algorithm, and loss rate-based algorithm are implemented to produce two subsets of AP, respectively, in the second step. The multi-objective optimization process then chooses the final subset of APs from the union of the two subsets.

III. METHODS

A. CONSTRUCTION OF INITIAL RADIO MAP

In this section, the proposed AP selection technique is presented. The matching algorithms used to predict the location of user are trained on a fingerprint database. To build the fingerprint database χ, M suitable points for positioning must be identified and these points will be assigned as the RPs. Typically, the RPs are strategically spaced in the deployment area. At each RP, RSS vectors are collected from K APs. The fingerprint database χ, which is made up of the RSS vector and its coordinate, can be expressed as

$$\chi = \begin{bmatrix} (l_{1,1}, l_{1,2}, \cdots, l_{1,C}) & (r_{1,1}, r_{1,2}, \cdots, r_{1,K}) \\ \vdots & \vdots \\ (l_{m,1}, l_{m,2}, \cdots, l_{m,C}) & (r_{m,1}, r_{m,2}, \cdots, r_{m,K}) \\ \vdots & \vdots \\ (l_{M,1}, l_{M,2}, \cdots, l_{M,C}) & (r_{M,1}, r_{M,2}, \cdots, r_{M,K}) \end{bmatrix}, \quad (2)$$

where $\boldsymbol{\chi} \in \mathbb{R}^{M\times(C+K)}$, $\boldsymbol{l}_m = [\, l_{m,1}\ l_{m,2}\ \cdots\ l_{m,C}\,]^T$ signifies the coordinate vector of RP m and C is the total number of components used to specify the coordinate vector, $\boldsymbol{r}_m = [\, r_{m,1}\ r_{m,2}\ \cdots\ r_{m,K}\,]^T$ represents the RSS vector that is measured at RP m, $r_{m,k}$ denotes the RSS from AP k at RP m, $m \in [1, M]$ and $k \in [1, K]$. A more compact form of (2) can be written as follows:

$$\chi = [\boldsymbol{L}\ \ \boldsymbol{R}], \tag{3}$$

where $\boldsymbol{L} = [\boldsymbol{l}_1\ \boldsymbol{l}_2\ \cdots\ \boldsymbol{l}_M\,]^T \in \mathbb{R}^{M\times C}$ and $\boldsymbol{R} = [\boldsymbol{r}_1\ \boldsymbol{r}_2\ \cdots\ \boldsymbol{r}_M\,]^T \in \mathbb{R}^{M\times K}$.

B. PROPOSED ACCESS POINT SELECTION SCHEME

Positioning systems that rely on a static radio map may not be sufficient to offer accurate localization, as static radio map fails to consider the temporal variation of the RSS [35], which are particularly prevalent in dynamic indoor environments. Without a doubt, if significant changes that may impact the RSS distribution take place to the indoor environment, e.g., layout change, the entries recorded in the fingerprint database will not be able to accurately represent the real-time RSS captured by the user device and therefore, reducing the accuracy of the positioning system. A method to ensure that the radio map constantly reflects the present wireless environment is by updating the radio map on a regular basis, but this requires a significant time and work load. Therefore, this work introduces a novel AP selection framework that can mitigate the issue discussed.

The main idea of the proposed AP selection algorithm involves periodic collection of RSS vectors from a smaller number of RPs. Instead of having to regularly update the radio map by re-collecting new RSS readings from all the predefined RPs, the AP selection scheme only employ a subset of the RPs, referred to as known points, to compute the changes that may occur to the received signal. The positioning system computes the discrepancy between the recently gathered RSS and the ones kept in the database and compares it with a threshold γ to identify and exclude unreliable APs from the location computation process. To configure γ, the system operator needs to assess the variations RSSs of different APs for the initial layout. When the indoor layout changes, the RSS deviations will increase further. Therefore, unreliable APs due to layout change can be detected by setting γ higher than the RSS variations observed in the initial layout.

The proposed AP selection scheme can be implemented in three distinct modes, namely the building-based AP selection (B-APS), floor-based AP selection (F-APS), and zone-based AP selection (Z-APS) modes. There is a significant distinction in how these three implementation modes calculate Euclidean RSS distances during the positioning phase. More specifically, for B-APS, the APs that are identified as unreliable by any known point within the building will be excluded in the calculation of Euclidean RSS distances between the received RSS and RSS for all the reference points (RPs) in the building. On the other hand, for F-APS and Z-APS, APs identified as unreliable by any known point within a specific floor or zone will not contribute to the calculation of Euclidean RSS distances between the received RSS and RSS for all RPs in that particular floor and zone, respectively. It is crucial to note that the concepts of the building-based, floor-based, and zone-based presented in our AP selection framework are entirely different from those reported in the existing literature, where these terms typically describe the level of location granularity that positioning techniques can predict, specifically, building, floor, and zone, respectively. For instance, in Track 3 of IPIN 2021 and IPIN 2022 [24], the floor detection techniques in the works showcased by Leviathan Team, Imec-waves Team, and X-Lab Team refer to the estimation of the floor of an unknown target. Further details on B-APS, F-APS and Z-APS will be explained in Section III-B-I, Section III-B-II, and Section III-B-III, respectively.

1) BUILDING-BASED AP SELECTION (B-APS)

The B-APS is implemented by selecting P known points from the sets of pre-defined RPs. Specifically, $P < M$ to reduce the cost of the system as more equipment will be needed with a greater number of known points. New RSS vectors will be collected periodically from these known points and these RSS vectors can be formulated as:

$$\tilde{\boldsymbol{\beta}}^k = [\, \tilde{\beta}_1^k\ \ \tilde{\beta}_2^k\ \ \tilde{\beta}_3^k\ \ \cdots\ \ \tilde{\beta}_P^k\,], \tag{4}$$

where $\tilde{\beta}_p^k$ represents the newly collected RSS from AP k at known point p, $1 \le k \le K$. Subsequently, the original RSS vectors stored during the construction of radio map is retrieved and is expressed as:

$$\boldsymbol{\beta}^k = [\, \beta_1^k\ \ \beta_2^k\ \ \beta_3^k\ \ \cdots\ \ \beta_P^k\,], \tag{5}$$

where β_p^k, $\beta_p^k \in \boldsymbol{R}$, signifies the RSS from AP k at known point p recorded in the existing fingerprint database, $1 \le k \le K$. Then, the difference between the newly collected RSS from AP k and original RSS recorded in the database is computed by:

$$\boldsymbol{\delta}^k = \left|\tilde{\boldsymbol{\beta}}^k - \boldsymbol{\beta}^k\right| = [\, \delta_1^k\ \ \delta_2^k\ \ \delta_3^k\ \ \cdots\ \ \delta_P^k\,] \tag{6}$$

Given a threshold γ, an AP will only be utilized during the location computation process if it satisfies the following condition:

$$\delta_p^k \le \gamma, \quad 1 \le p \le P \tag{7}$$

Consequently, during localization, the total AP used will be reduced to K'. Fig. 1 illustrates the flowchart of B-APS.

2) FLOOR-BASED AP SELECTION (F-APS)

Since this work focused on evaluating the indoor positioning system in a multi-story building, F-APS is proposed whereby the localization area is separated by floors. The flowchart of F-APS is shown in Fig. 2. Considering a building with F floors, the radio map is constructed by assigning M_f RPs at each floor, resulting in $M = \sum_{f=1}^{F} M_f$. Additionally, each

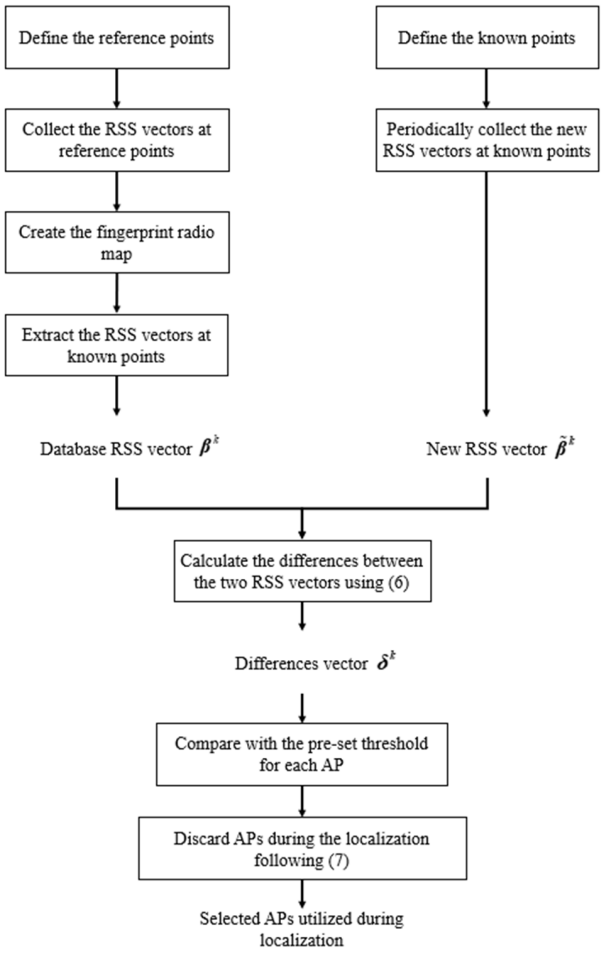

FIGURE 1. Flowchart of B-APS.

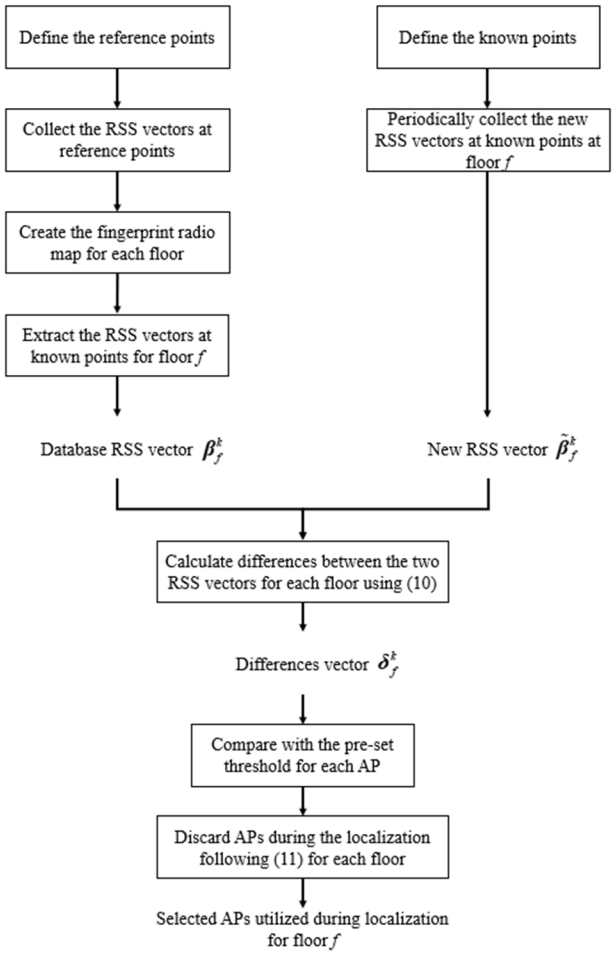

FIGURE 2. Flowchart of F-APS.

floor contains P_f known points, $P_f < M_f$, where new RSS is obtained periodically. The total number of known points in the entire localization area will be $P_1 + P_2 + \ldots + P_F = P < M$. The new RSS vectors obtained at floor f is expressed as

$$\tilde{\boldsymbol{\beta}}_f^k = [\,\tilde{\beta}_{f,1}^k \;\; \tilde{\beta}_{f,2}^k \;\; \tilde{\beta}_{f,3}^k \;\; \cdots \;\; \tilde{\beta}_{f,P_f}^k\,], \tag{8}$$

where $\tilde{\beta}_{f,p}^k$ represents the newly collected RSS from AP k at known point p, $1 \le k \le K$ and $1 \le f \le F$. The original RSS vectors stored during the construction of radio map for floor f is retrieved and is expressed as:

$$\boldsymbol{\beta}_f^k = [\,\beta_{f,1}^k \;\; \beta_{f,2}^k \;\; \beta_{f,3}^k \;\; \cdots \;\; \beta_{f,P_f}^k\,], \tag{9}$$

where β_p^k, $\beta_{f,p}^k \in \boldsymbol{R}$, indicates the RSS from AP k at known point p recorded in the existing fingerprint database, $1 \le k \le K$ and $1 \le f \le F$. Subsequently, the difference between the newly collected RSS from AP k and original RSS recorded in the database for known points of the same floor is computed by

$$\boldsymbol{\delta}_f^k = \left|\tilde{\boldsymbol{\beta}}_f^k - \boldsymbol{\beta}_f^k\right| = [\,\delta_{f,1}^k \;\; \delta_{f,2}^k \;\; \delta_{f,3}^k \;\; \cdots \;\; \delta_{f,P_f}^k\,] \tag{10}$$

By setting a threshold γ, an AP will only be utilized during the fingerprint matching process if it satisfies the following condition:

$$\delta_{f,p}^k \le \gamma, \quad 1 \le p \le P_f \tag{11}$$

Consequently, the total AP employed for localization in floor f will be reduced to K_f'.

3) ZONE-BASED AP SELECTION (Z-APS)

Unlike F-APS, Z-APS does not divide the localization area based on the number of floors. Instead, it separates the localization area into Z smaller zones. The flowchart of Z-APS is depicted in Fig. 3. From the pre-established RPs, P_z points are designated as known points in zone z where RSS are collected on a regular basis and the RSS vectors can be written as

$$\tilde{\boldsymbol{\beta}}_z^k = [\,\tilde{\beta}_{z,1}^k \;\; \tilde{\beta}_{z,2}^k \;\; \tilde{\beta}_{z,3}^k \;\; \cdots \;\; \tilde{\beta}_{z,P_z}^k\,], \tag{12}$$

where $\tilde{\beta}_{z,p}^k$ represents the newly collected RSS from AP k at known point p located at zone z, $1 \le k \le K$ and $1 \le z \le Z$. The RSS registered in the database for zone z is extracted and can expressed as:

$$\boldsymbol{\beta}_z^k = [\,\beta_{z,1}^k \;\; \beta_{z,2}^k \;\; \beta_{z,3}^k \;\; \cdots \;\; \beta_{z,P_z}^k\,], \tag{13}$$

where $\beta_{z,p}^k$, $\beta_{z,p}^k \in \boldsymbol{R}$ represents the RSS from AP k at known point p located in zone z recorded in the existing fingerprint

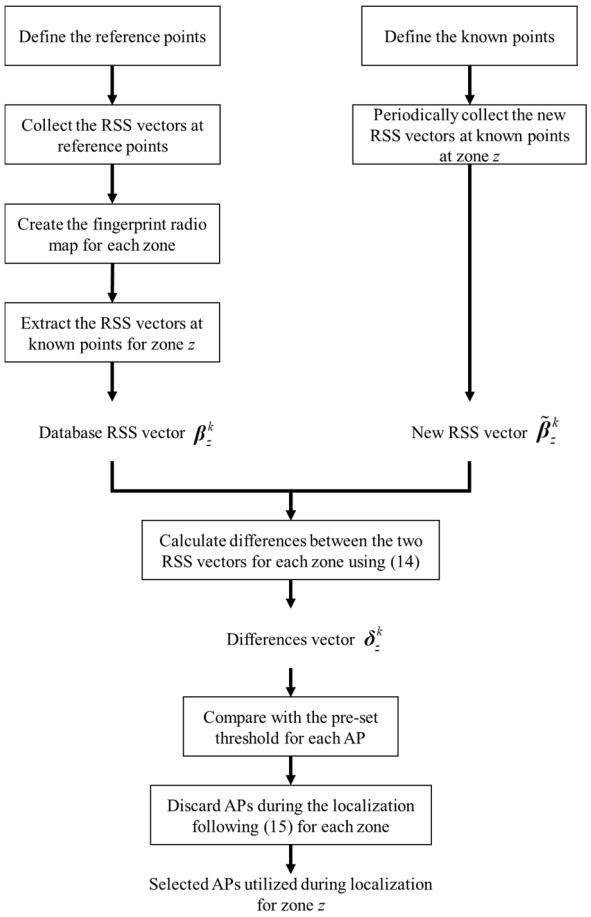

FIGURE 3. Flowchart of Z-APS.

database, $1 \leq k \leq K$ and $1 \leq z \leq Z$. Afterwards, the difference between the newly collected RSS and RSS recorded in the database for known points of the same zone is calculated through

$$\boldsymbol{\delta}^k = \left| \tilde{\boldsymbol{\beta}}^k - \boldsymbol{\beta}^k \right| = [\, \delta_1^k \;\; \delta_2^k \;\; \delta_3^k \;\; \cdots \;\; \delta_{P_z}^k \,] \tag{14}$$

Similar to B-APS and F-APS, a threshold γ is set. By comparing values calculated in (14) with the pre-set γ, an AP will only be utilized during the location computation process for zone z if it satisfies the following condition:

$$\delta_{z,p}^k \leq \gamma, \quad 1 \leq p \leq P_z \tag{15}$$

Consequently, the total AP in used by each zone during localization will be reduced to K_z'.

C. ONLINE LOCALIZATION

Fig. 4 illustrates the flowchart of the online localization process of the indoor positioning system During the online query phase, the user device will measure the RSS vector from its unknown position u. The received RSS vector is described as

$$\boldsymbol{r}_u = [\, r_{u,1} \;\; r_{u,2} \;\; \cdots \;\; r_{u,K} \,], \tag{16}$$

where $r_{u,k}$ is the RSS collected from AP k at unknown point u.

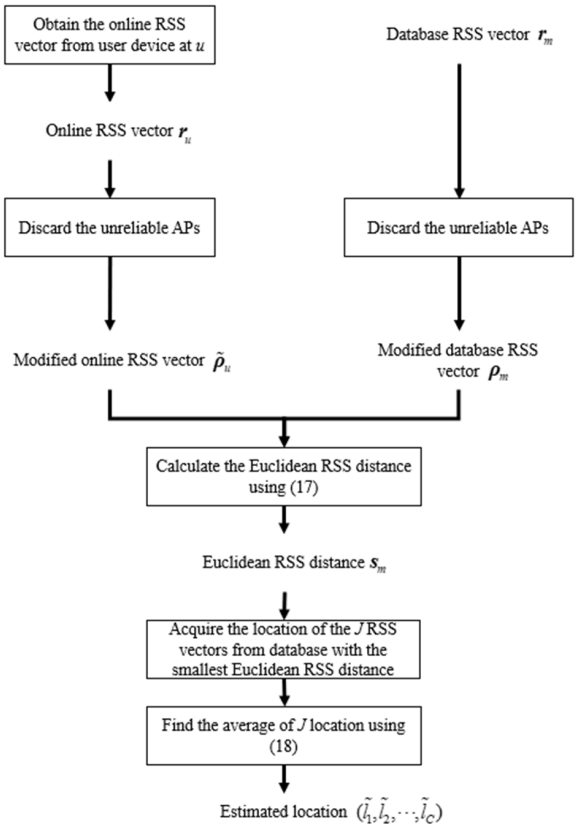

FIGURE 4. Flowchart of online localization.

For position estimation, the Euclidean RSS distance of the RSS between the unknown test point and the training point in the database needs to be computed. As mentioned in Section III-B, the number of APs used during localization is reduced following the AP selection strategies due to the unreliable APs. For B-APS the number of APs were reduced from K to K', whereas the number APs utilized during localization is reduced to K_f' in each floor and K_z' in each zone for F-APS and Z-APS, respectively. For simplicity, the total number of AP used during localization will be denoted by $\tilde{K}$ in this section. Thus, modified vectors of RSS are required during the computation of Euclidean RSS distance. By deleting the columns that contain the unreliable APs, both online RSS vector $\boldsymbol{r}_u$ and database RSS vector $\boldsymbol{r}_m$, $m \in [1, M]$, are transformed into the modified online RSS vector $\tilde{\boldsymbol{\rho}}_u = [\, \tilde{\rho}_{u,1} \;\; \tilde{\rho}_{u,2} \;\; \cdots \;\; \tilde{\rho}_{u,\tilde{K}} \,]$ and modified database RSS vector $\boldsymbol{\rho}_m = [\, \rho_{m,1} \;\; \rho_{m,2} \;\; \cdots \;\; \rho_{m,\tilde{K}} \,]$, respectively. The following is used to compute the Euclidean RSS distance between RSS of the unknown test point and the m-th entry in the database.

$$s_m = \left[\sum_{k=1}^{\tilde{K}} (\tilde{\rho}_{u,k} - \rho_{m,k})^2 \right]^{\frac{1}{2}}, \tag{17}$$

where $\tilde{\rho}_{u,k}$ is the RSS from AP k at unknown point u acquired from the modified online RSS vector and $\rho_{m,k}$ is the RSS

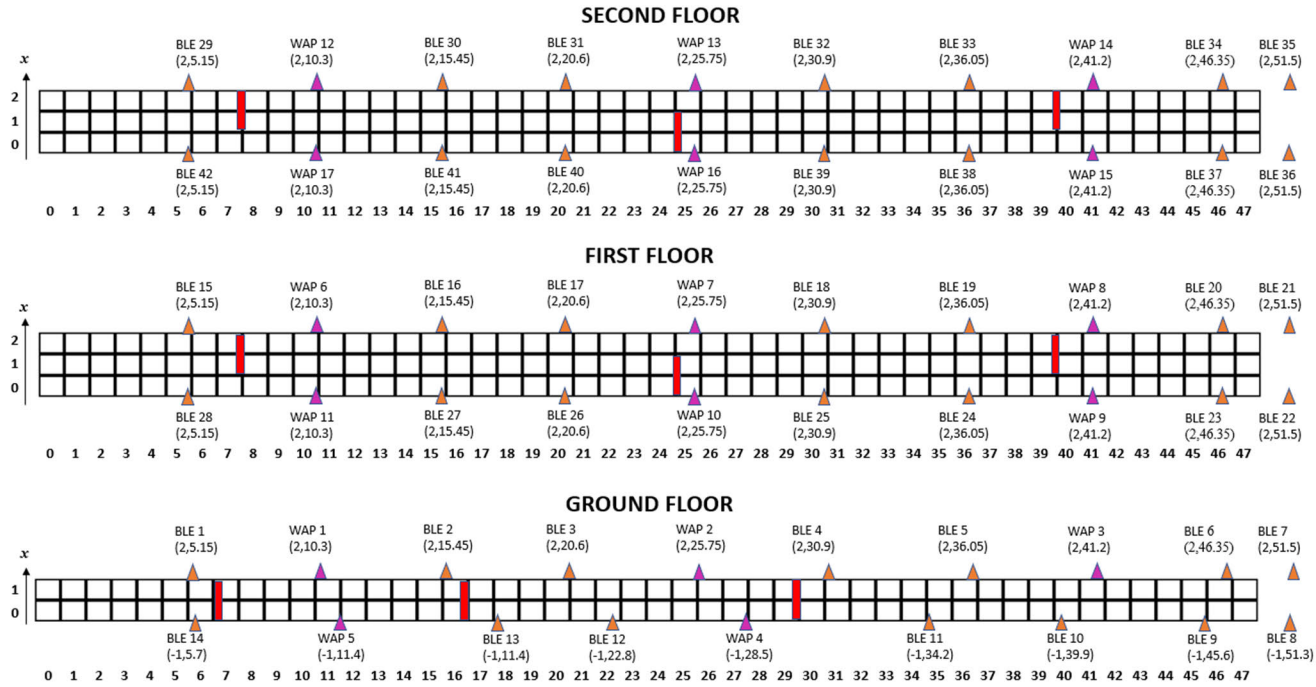

FIGURE 5. Layout of the indoor environment with boards placed in the localization area.

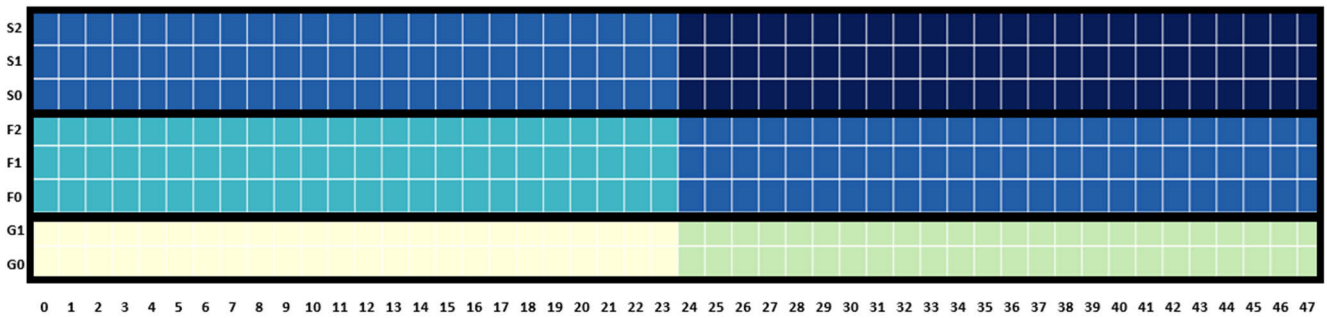

FIGURE 6. Sub-regions of the indoor localization area for Z-APS with 6 zones.

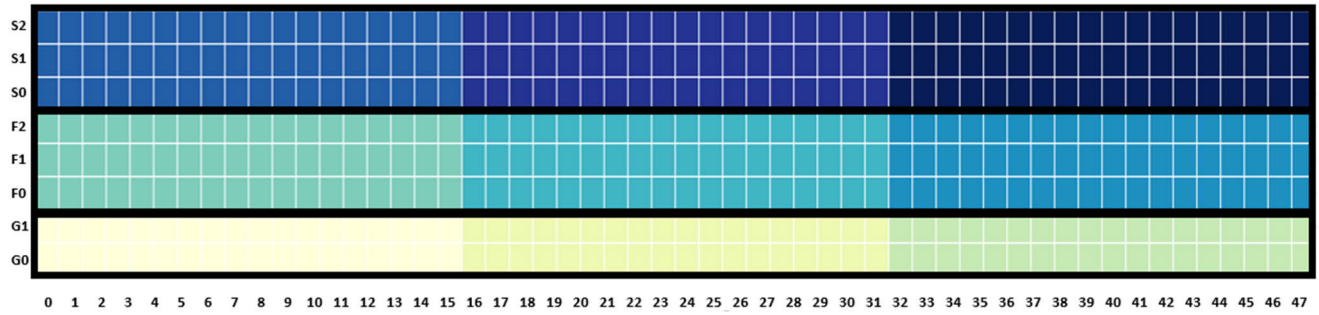

FIGURE 7. Sub-regions of the indoor localization area for Z-APS with 9 zones.

from AP k at RP m obtained from the modified database RSS vector.

The Euclidean RSS distance calculated can be denoted as $\boldsymbol{s} = [\, s_1 \; s_2 \; \cdots \; s_M \,]$. After obtaining the Euclidean RSS distance between the online RSS vector and the RSS vectors from the database, J number of RSS vectors from the database with the smallest Euclidean RSS distance will be searched and the location that was tagged to the RSS vectors

will be obtained. Finally, to find the position of the target, the average between these J acquired location is computed using

$$(\tilde{l}_1, \tilde{l}_2, \cdots, \tilde{l}_C) = \frac{\sum_{j=1}^{J} \left(l_{j,1}, l_{j,2}, \cdots, l_{j,C}\right)}{J}, \quad (18)$$

where $\left(l_{j,1}, l_{j,2}, \cdots, l_{j,C}\right)$ represents the location coordinate of the j-th nearest entries in the database, $c \in [1, C]$.

IV. EXPERIMENTAL ENVIRONMENTS AND DATASETS

In this section, we detail the experimental environments and described the datasets used for simulating the positioning systems. The proposed AP selection schemes are evaluated using the Hybrid Data Layout Change (HDCL) [36] dataset, comprising real measurements from a campaign that is conducted at the Faculty of Engineering (FOE), Multimedia University, Cyberjaya, Malaysia. The dataset encompasses the corridors of three floors, i.e., ground floor, first floor and second floor, each with a floor-to-floor height of 3.5 m. The ground floor has dimensions of 51.5 m × 2.1 m whereas the second and third floor both have dimensions of 51.5 m × 2.7 m. A total of 384 RPs was arranged in the localization space, where they were evenly spaced 1 m apart from each other. Since the ground floor has a smaller area compared to the first and second floors, it contains only 96 RPs, while each of the first and second floors contain 144 RPs. The deployment involved 42 BLE beacons and 17 Wi-Fi APs (WAPs). In total, the database comprises 59 RSS values and 3 labeled attributes about the fingerprint which are the x-coordinate, y-coordinate, and z-coordinate of the RPs. The z-coordinate of the RPs located on ground floor, first floor, and second floor are 0, 3.5 and 7, respectively. To construct the fingerprint radio map, a total of 20 RSS samples were collected at each RP and for the testing dataset, an additional 10 samples were collected at each RP. The RSS samples were collected in two different layouts, one of which will be referred to as the original layout and the other as the modified layout. The difference between the original layout and the modified layout is that the modified layout contains multiple boards with a height of 1.8 m, a length of 1.5 m and a thickness of 0.01 m, which act as a barrier in the indoor environment to induce the permanent and transient change for dynamic environment. Fig. 5 illustrates the layout of the calibration site which also includes the placement of partition board.

Since the proposed Z-APS algorithms is tested with different number of zones, Figs. 6 and 7 are provided to clearly illustrates the zones and their boundaries after the indoor environment has been divided into 6 and 9 zones, respectively. From the figures, it shows that each floor has the same number of zones. In this work, the AP selection algorithm is evaluated with varying number of known points. Importantly, we have fixed the known point such that it is evenly spread throughout the localization region so that the system is able to register the changes in RSS of the entire space. Table 1 displays the coordinates of known points with varying number of known points.

TABLE 1. Coordinates of known points.

Total number of known points	Coordinates of known points
3	(0,23,0), (1,23,3.5), (1,23,7)
6	(0,11,0), (0,35,0), (1,11,3.5), (1,35,3,5), (1,11,7), (1,35,7)
9	(0,7,0), (0,23,0), (0,39,0), (1,7,3.5), (1,23,3.5), (1,39,3.5), (1,7,7), (1,23,7), (1,39,7)
12	(0,5,0), (0,17,0), (0,29,0), (0,41,0), (1,5,3.5), (1,17,3.5), (1,29,3.5), (1,41,3.5), (1,5,7), (1,17,7), (1,29,7), (1,41,7)
18	(0,4,0), (0,12,0), (0,20,0), (0,28,0), (0,36,0), (0,44,0), (1,4,3.5), (1,12,3.5), (1,20,3.5), (1,28,3.5), (1,36,3.5), (1,44,3.5), (1,4,7), (1,12,7), (1,20,7), (1,28,7), (1,36,7), (1,44,7)
36	(0,1,0), (0,5,0), (0,9,0), (0,13,0), (0,17,0), (0,21,0), (0,25,0), (0,29,0), (0,33,0), (0,37,0), (0,41,0), (0,45,0), (1,1,3.5), (1,5,3.5), (1,9,3.5), (1,13,3.5), (1,17,3.5), (1,21,3.5), (1,25,3.5), (1,29,3.5), (1,33,3.5), (1,37,3.5), (1,41,3.5), (1,45,3.5), (1,1,7), (1,5,7), (1,9,7), (1,13,7), (1,17,7), (1,21,7), (1,25,7), (1,29,7), (1,33,7), (1,37,7), (1,41,7), (1,45,7)

V. RESULTS AND DISCUSSION

In this section, a thorough analysis of the performance of the proposed and baseline techniques is provided. Since the floor-to-floor distance of the building is 3.5 m, the floor level is replaced with 0 m, 3.5 m and 7.0 m for the ground floor, first floor and second floor, respectively, in the calculation of the 3D average positioning error. The 3D average positioning error can be calculated as follows

$$\varepsilon = \frac{1}{N} \sum_{n=1}^{N} \sqrt{(\tilde{x}_n - x_n)^2 + (\tilde{y}_n - y_n)^2 + (\tilde{z}_n - z_n)^2}, \quad (19)$$

where N represents the total number of test samples, $(\tilde{x}_n, \tilde{y}_n, \tilde{z}_n)$ and (x_n, y_n, z_n) are the predicted and the actual coordinates of the n-th test point, respectively.

Table 2 offers insights into the floor accuracy η and the average positioning error ε of various techniques considered where each scheme is assessed using γ in the range of 22.5 dBm to 40 dBm, with a 2.5 dBm increment. In the table, the total number of sub-regions established for the proposed AP selection schemes is denoted by Q. Without implementing the proposed AP selection scheme, the positioning system can achieve a floor accuracy of 99.56%. In general, the floor accuracy of the system can be further improved and even exhibit a 100% floor accuracy by the implementation of the AP selection scheme as shown in Table 2.

A more comprehensive understanding of the effectiveness of the AP selection technique can be gained by examining the average positioning error of the positioning system. A positioning error of 4.455 m is attained when the positioning system is executed without the implementation of the proposed AP selection scheme. As evident in Table 2, the system with Z-APSs generally attain the lowest positioning

TABLE 2. The localization performance of the proposed AP selection strategies.

Implementation mode	Q	P	γ (dBm)															
			22.5		25		27.5		30		32.5		35		37.5		40	
			η(%)	ε(m)	η(%)	ε(m)	η(%)	ε(m)	η(%)	ε(m)	η(%)	ε(m)	η(%)	ε(m)	η(%)	ε(m)	η(%)	ε(m)
B-APS	1	3	100	3.1693	100	3.2623	100	3.2623	100	3.8308	100	3.8308	100	3.4644	100	3.8834	99.74	3.8174
		6	99.97	3.6194	100	3.7327	100	4.052	100	3.7953	100	3.9589	99.92	4.208	99.92	4.208	99.87	4.5799
		9	99.97	3.6337	99.97	3.3988	100	3.2623	100	3.8939	100	3.8308	100	3.4644	100	3.8834	99.74	3.8174
		12	99.97	4.6108	99.97	4.0697	100	3.4158	100	4.0996	100	3.5258	100	3.5258	100	3.4264	99.74	4.4192
		18	99.97	4.7991	99.97	4.5606	100	3.6235	100	3.54	100	4.0773	100	3.4649	100	3.8951	100	4.709
		36	99.97	5.1634	99.97	4.6398	99.97	4.0322	100	4.1278	100	4.0773	100	4.1005	100	3.8438	100	4.709
F-APS	3	3	100	3.2076	100	3.1937	100	3.4824	100	3.6686	100	3.6686	100	3.461	100	3.9766	99.92	3.8342
		6	100	3.1989	100	3.1618	100	3.0192	99.95	3.5211	100	3.7477	100	4.1739	100	4.1739	99.87	4.5857
		9	100	3.1882	100	3.0854	100	3.4824	99.97	3.6964	100	3.6686	100	3.461	100	3.9766	99.92	3.8342
		12	100	3.0114	100	3.0491	100	2.9611	100	3.1143	100	3.2068	100	3.2068	100	3.378	99.74	4.5835
		18	100	3.3365	100	3.3786	100	3.2659	100	3.1539	99.48	3.4641	99.9	3.3269	100	3.8179	100	4.7781
		36	100	3.4723	100	3.1921	100	3.2358	99.97	3.4063	99.48	3.4641	100	3.5731	100	3.6451	100	4.7781
Z-PS	6	6	100	3.2295	100	3.2271	100	3.317	100	3.7498	100	3.7882	99.9	4.0894	99.9	4.0894	99.77	4.4495
		12	100	3.0517	100	3.382	100	3.2475	100	3.1452	100	3.0929	100	3.1935	100	3.5083	99.71	4.8264
		18	100	3.2937	100	3.2301	100	3.3454	100	3.1812	100	3.2283	100	3.5054	100	3.7127	99.92	4.8509
		36	100	3.0984	100	3.2964	100	3.3202	100	3.629	100	3.4708	100	3.6262	100	3.7178	99.92	4.8509
	9	9	100	2.8479	100	2.9301	100	3.0089	100	3.2505	100	3.0348	99.92	3.0376	99.69	3.1342	99.56	3.7475
		18	100	2.7179	100	2.6907	100	3.1524	100	2.9472	100	2.9575	100	3.1132	100	3.2097	99.77	3.7118
		36	100	2.6882	100	2.7642	100	3.0479	100	3.1746	100	2.9886	100	3.0157	100	3.1423	99.77	3.7118

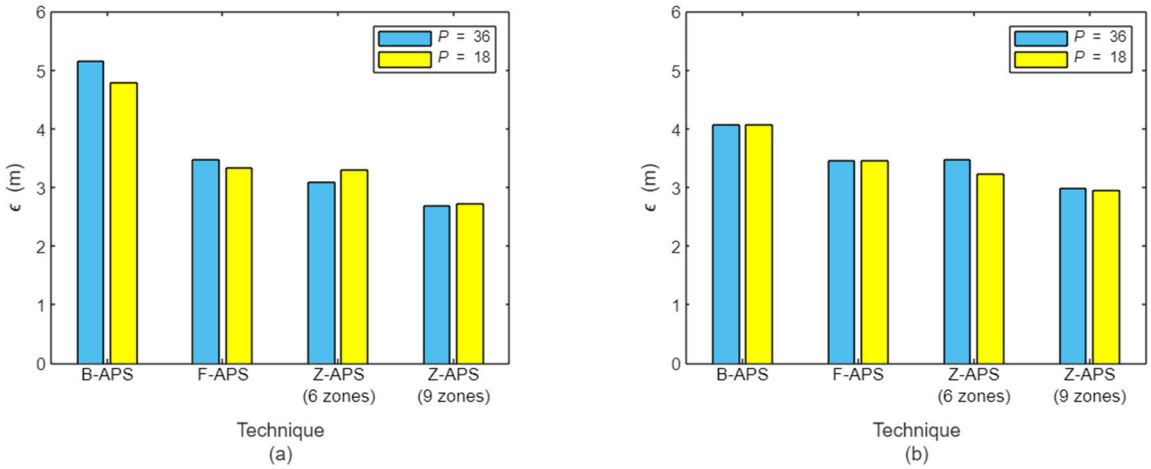

FIGURE 8. Average positioning errors of the proposed AP selection schemes for (a) $\gamma = 22.5$ dBm and (b)$\gamma = 32.5$ dBm.

error, followed by the system with F-APS and the B-APS. Quantitatively, it is observed that Z-APS with 9 zones, $P = 36$ and $\gamma = 22.5$ dBm yields the lowest positioning error of 2.6882 m. With identical P and γ, the average positioning error increases to 3.0984 m as the number of zones decreases from 9 to 6. On the other hand, F-APS records an average positioning error of 3.4723 m, while B-APS exhibits the highest average positioning error of 5.1634 m. This performance trend is attributed to the variation in Q in the localization area that depends on the approach used; for example, Z-APS have both 9 and 6 sub-regions, whereas F-APS and B-APS have 3 and 1 sub-region, respectively. Thus, it is evident that the scheme with the lowest positioning error tends to be the one that employs a greater Q.

To further substantiate this claim, Fig. 8(a) illustrates that the average positioning error of the proposed AP selection schemes increases in the following sequence: Z-APS with 9 zones, Z-APS with 6 zones, F-APS and B-APS. The same trend is also observed in Fig. 8(b) when γ is increased to 32.5 dBm. The rationale behind a larger Q resulting in smaller error lies in the finer division of the localization area into smaller sub-regions. The finer granularity decreases the likelihood of eliminating APs that may be suboptimal for a small number of known points in the region, particularly those near the edges of the sub-regions, but beneficial for the majority of known points in the same region. It is also worth highlighting that the proposed AP selection technique not only results in enhanced floor classification accuracies and reduced average positioning errors compared to the baseline approach, but also lead to lower computational complexities in the online localization phase. This is due to reason that the computational complexity of the machine learning based positioning technique is proportional the number of APs considered in online localization phase.

To facilitate comparison with baseline positioning system, Fig. 9(a) shows the performance gain of the AP selection schemes at $\gamma = 22.5$ dBm with $P = 18$ and $P = 36$, while Fig. 9(b) depicts the performance gain at $\gamma = 32.5$ dBm with

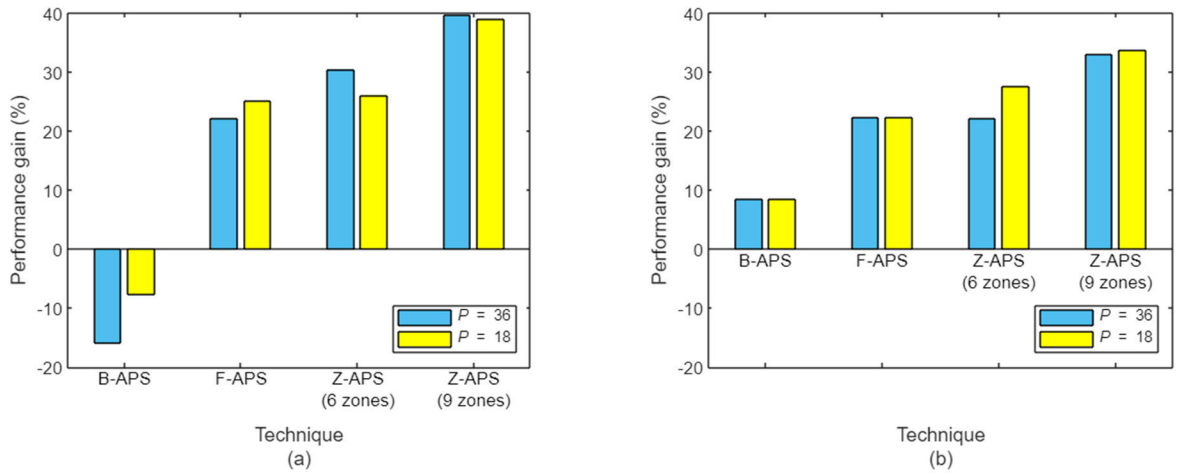

FIGURE 9. Performance gains of the proposed AP selection schemes over the baseline technique in terms of average positioning error for (a) $\gamma = 22.5$ dBm and (b) $\gamma = 32.5$ dBm.

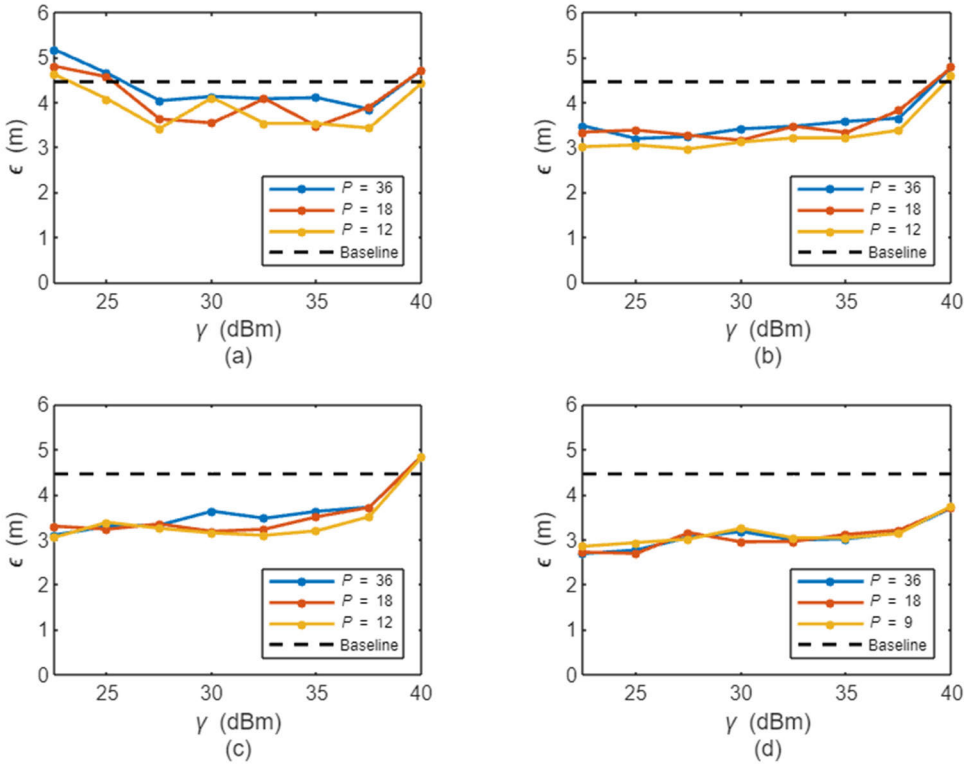

FIGURE 10. Average position errors against γ for (a) B-APS, (b) F-APS, (c) Z-APS with 6 zones and (d) Z-APS with 9 zones.

$P = 18$ and $P = 36$. It can be observed from Fig. 9 that both F-APS and Z-APS outperform the baseline technique in terms of average positioning error for both γ settings. When γ is set to 32.5 dBm, Z-APS with 9 zones yields the lowest positioning error and displays the highest performance gain. This is followed by Z-APS with 6 zones, F-APS and lastly B-APS. However, at $\gamma = 22.5$ dBm, B-APS exhibits a degradation of 15.90% and 7.72% compared to the baseline technique for $P = 36$ and $P = 18$, respectively, because the system might not have sufficient APs during localization when γ is low.

Fig. 10 illustrates the average positioning error of the AP selection scheme for γ from 22.5 dBm to 40 dBm. In general, the proposed technique with different implementation modes exhibit similar performance trend except for B-APS. More explicitly, for the same value of P, a very low positioning

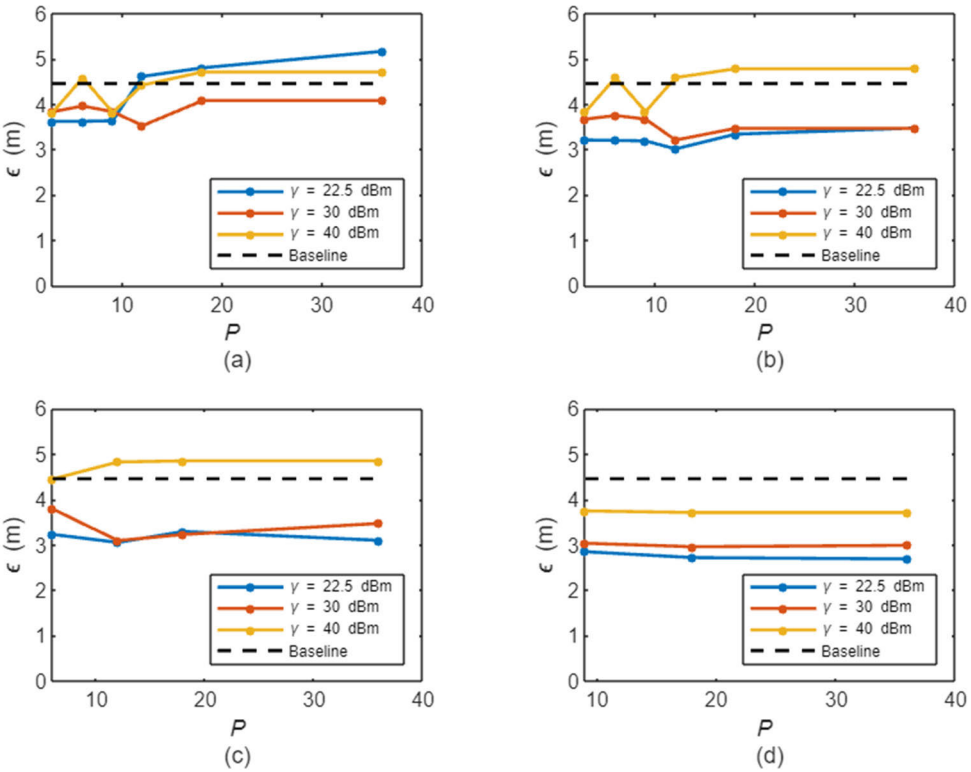

FIGURE 11. Average position error against P (a) B-APS, (b) F-APS, (c) Z-APS with 6 zones and (d) Z-APS with 9 zones.

error can be observed at $\gamma = 22.5$ dBm for the F-APS and Z-APS techniques and as γ increases beyond 35 dBm, there is a noticeable rise in positioning errors. This is due to the reason that a higher threshold setting permits APs with larger RSS deviations to be included in estimation of the position, making the system less reliable. Hence, an excessively large threshold setting is typically not ideal for the proposed AP selection scheme. As for B-APS, a high positioning error can also be observed at $\gamma = 40$ dBm. However, the scheme's performance differs slightly since it produces the highest localization error when γ is set to 22.5 dBm. This results in average positioning errors of 5.1634 m, 4.7991 m and 4.6108 m for $P = 36$, $P = 18$ and $P = 12$, respectively, which are worse than that of the baseline. The reason behind the B-APS's large errors at low γ can be explained as follows: For a lower threshold, the discrepancy between the RSS from user device and the database must be small to allow the AP to be used during localization. Since there are multiple known points throughout the localization area, there is a higher possibility that the B-APS algorithm identify different sets of unstable APs for each known points. Consequently, many of the APs will be discarded during localization when γ is low, leading to insufficient AP for accurate positioning. In comparison to F-APS and Z-APS counterparts, a larger threshold is required for the B-APS approach to outperform the baseline technique. More specifically, B-APS exhibits a positioning error lower than that of the baseline when γ is in the range of 27.5 dBm to 37.5 dBm.

Having examined the impact of γ on the localization performance of the AP selection schemes, the effects of P are depicted in Fig. 11. As observed, the overall trend in Figs. 11 is well-aligned with the previous findings in Figs. 10. It is observed that across varying P, the largest threshold observes the highest error, while the lowest threshold recorded the lowest error. The effects of P on the performance of the AP selection scheme, however, are not as clear since a consistent trend cannot be observed when P is varied. Nevertheless, for B-APS, a lower P value is preferable since many known points would lead to the possibility of insufficient localization information especially when the unstable APs detected at different known points are different. On the other hand, as the number of sub-regions for the AP selection scheme increases, a larger P value might be advantageous. For instance, the Z-APS with 9 zones at $\gamma = 22.5$ dBm yields the lowest error positioning error of 2.6882 m when P is set to 36. This is because Z-APS with 9 zones has more sub-regions than B-APS, requiring more known points to ensure that each has sufficient known points to effectively detect the APs, which could negatively impact the localization performance of the sub-region.

Fig. 12 illustrates the spatial distribution of positioning errors across the localization area for the baseline positioning system, which operates without an AP selection scheme. In this study, a positioning error exceeding 7 m is deemed a failure in locating the test point. The findings reveal that the baseline scheme fails to locate 15.63% of the test points.

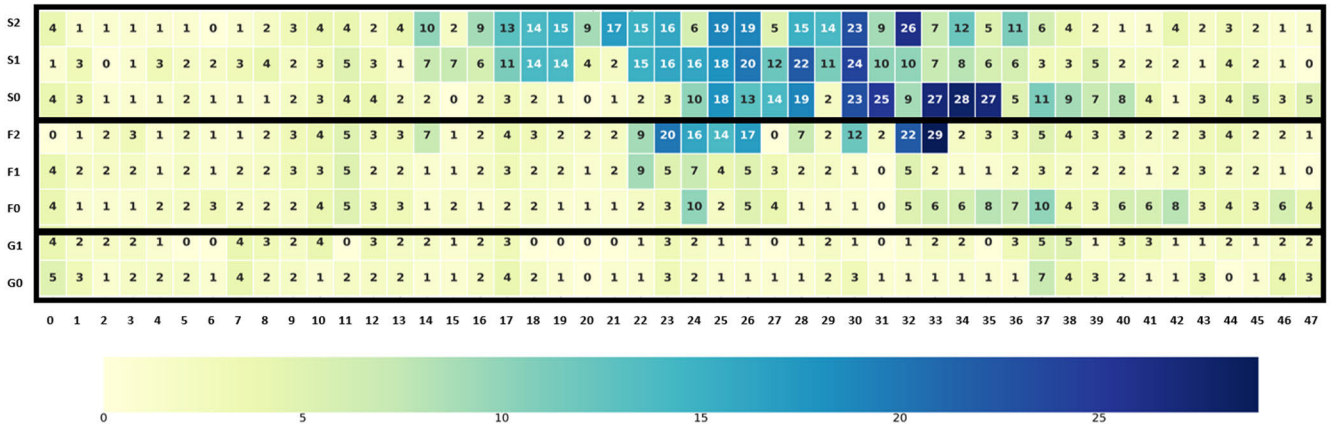

FIGURE 12. Spatial distribution of positioning errors of the indoor positioning system without AP selection schemes.

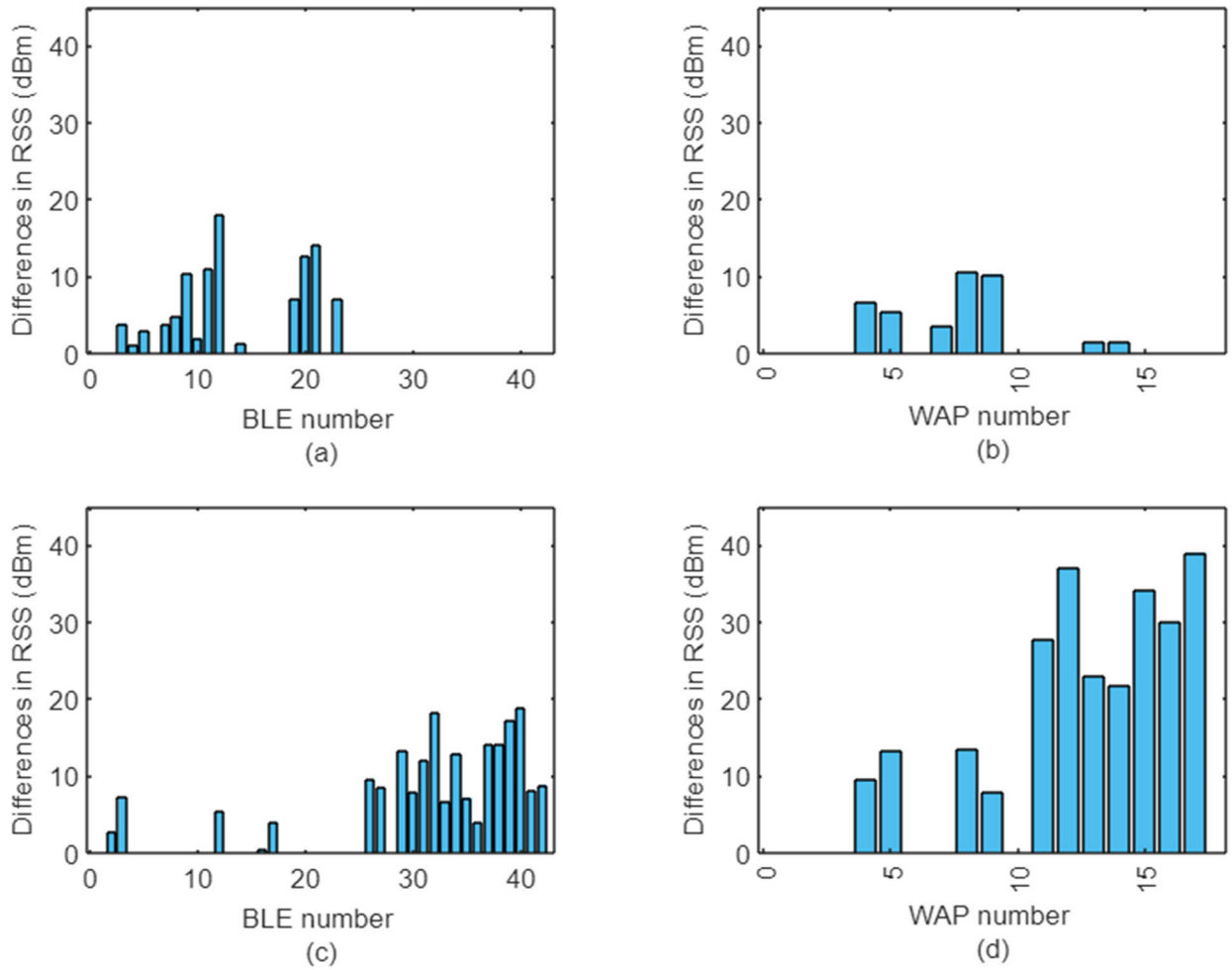

FIGURE 13. RSS variations induced by layout change, collected at (a) coordinate (0, 31, 0) on the ground floor from BLEs, (b) coordinate (0, 31, 0) on the ground floor from WAPs, (c) coordinate (0, 31, 7) on the second floor from BLEs and (d) coordinate (0, 31, 7) on the second floor from WAPs.

The heatmap in Fig. 7 further demonstrates that majority of the test points, where the system fails to identify their coordinates, are situated on the second floor of the building. More specifically, 32.63% of the test points on the second floor exhibit positioning errors surpassing 7 m, while none of test points on the ground floor exceed this threshold.

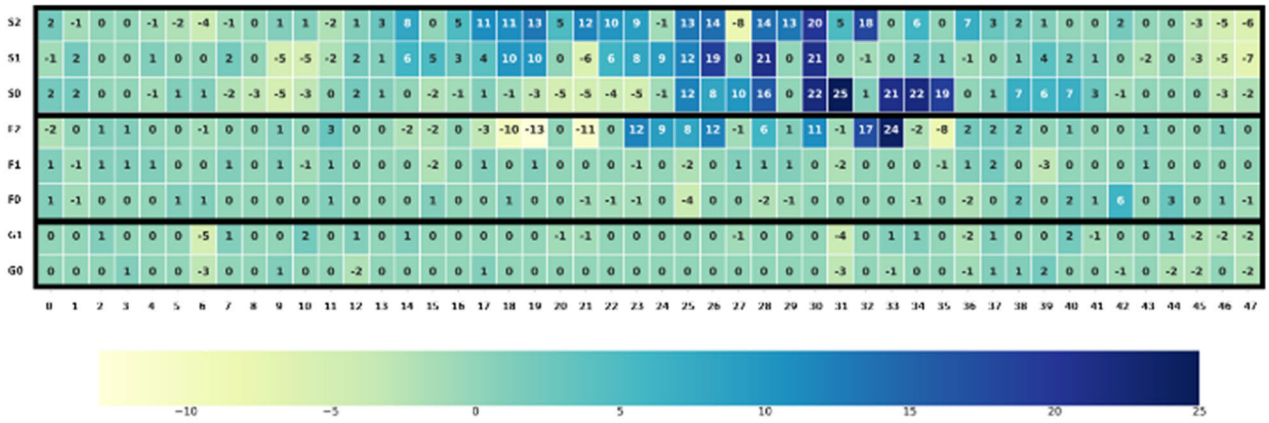

FIGURE 14. Spatial distribution of differences in average positioning error between the baseline technique and B-APS with $\gamma = 22.5$ dBm and $P = 3$.

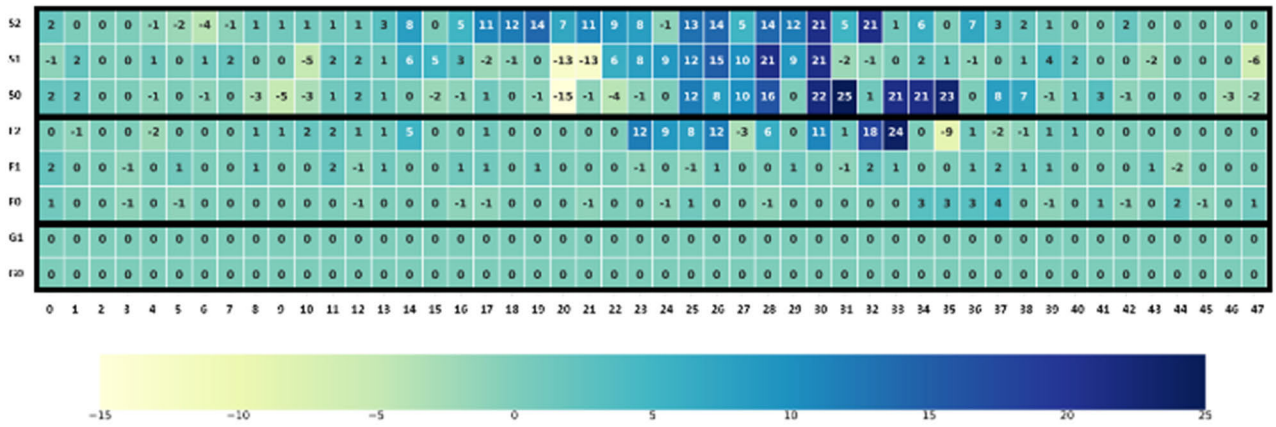

FIGURE 15. Spatial distribution of differences in average positioning error between the baseline technique and F-APS with $\gamma = 27.5$ dBm and $P = 12$.

To shed light on the reasons behind the baseline system's inferior performance on the third floor in comparison to the ground floor, the variations in RSSs caused by the layout change is investigated. In Fig. 13, we examine the RSS variation at coordinate (0, 31, 0) on the ground floor, which has an error of 1 m, and compare them with those at (0, 31, 7) on the second floor, where a more substantial error of 25 m is observed. The increased positioning error for coordinate (0, 31, 7) on the second floor, relative to coordinate (0, 31, 0) on the ground floor, is attributed to signals from the APs at the coordinate (0, 31, 0) being less adversely affected by the partitioning boards than at coordinate (0, 31, 7). For example, the RSS differences of affected WAP for coordinate (0, 31, 7) are higher than 20 dBm. In comparison, the RSSs from the WAPs detected at coordinate (0, 31, 0) on the ground floor only deviate by around 10 dBm.

It is also noteworthy that the APs substantially impacted by the layout change are generally in close proximity to the test points. For example, in Fig. 13, the most significant discrepancy in RSS values collected at coordinate (0, 31, 0) on the ground floor is evident with BLE 12, situated at (−1, 22.8, 0). As for coordinate (0, 31, 7) on the second floor, the signals from WAPs 11 – 17 are observed to be the most affected by the layout change. WAPs 12 –17 are all on the same floor as coordinate (0, 31, 7), except for WAP 11. This is because for APs distant from the test points, signal attenuation dominates, resulting in weak signals received by the test points during layout change or without layout change. Conversely, for APs in close proximity to the test points, signal attenuation due to path loss becomes less pronounced, causing RSSs received from these APs highly sensitive to the environmental dynamics. Consequently, the RSS variations for distant APs are smaller than those for the nearer ones.

To demonstrate the effectiveness of the proposed AP selection strategies in mitigating the impact of layout change on the localization performance, the heatmaps of the disparities in average positioning error between the baseline system and the proposed AP selection schemes are displayed in Figs. 14 – 17. For each of the proposed AP selection schemes, only the results for the configuration with the lowest average positioning error are presented. Specifically, the γ for both Z-APS techniques are 22.5 dBm, while the γ

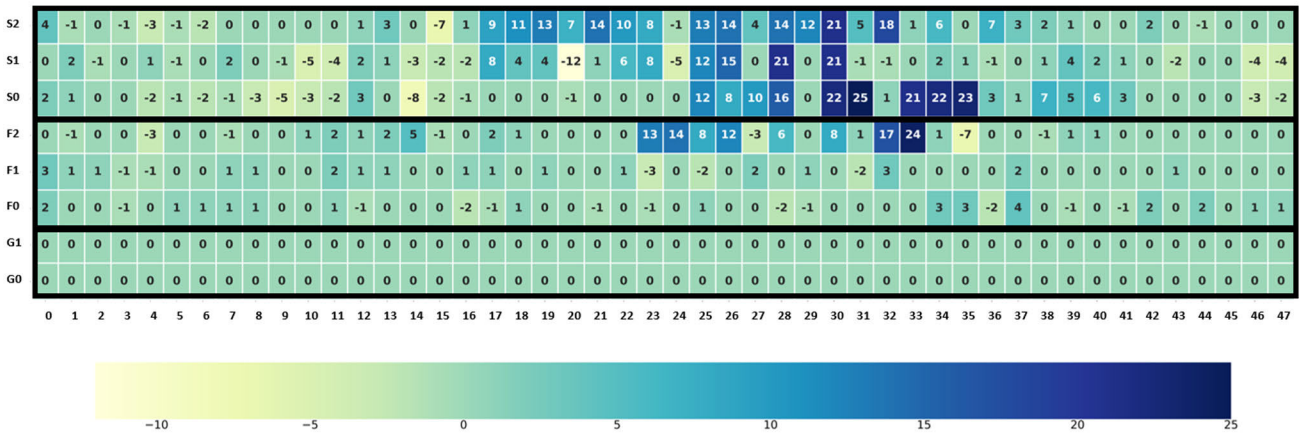

FIGURE 16. Spatial distribution of differences in average positioning error between the baseline technique and Z-APS with 6 zones, $\gamma = 22.5$ dBm and $P = 12$.

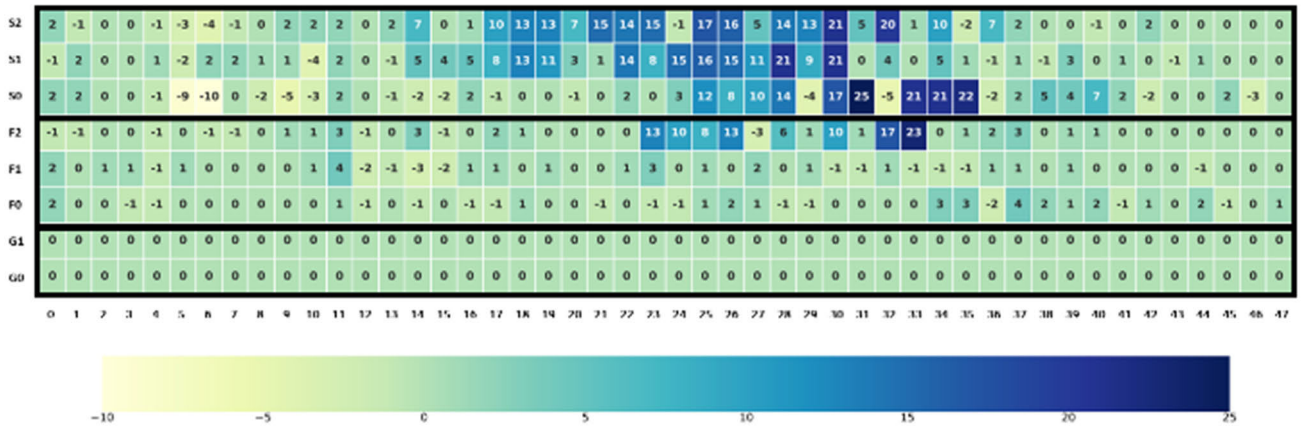

FIGURE 17. Spatial distribution of differences in average positioning error between the baseline technique and Z-APS with 9 zones, $\gamma = 22.5$ dBm and $P = 9$.

settings for F-APS and B-APS are 27.5 dBm and 22.5 dBm, respectively. On the other hand, the P for B-APS, F-APS, Z-APS with 6 zones and Z-APS with 9 zones are 3, 12, 12 and 9, respectively. In these heatmaps, a positive average positioning error difference implies that the proposed method has a lower positioning error while a negative value implies otherwise.

Upon analyzing Figs. 14 - 17, it is apparent that the second floor exhibits the highest number of significant positive differences in average positioning errors. Notably, at coordinate (0, 31, 7) on the second floor, the most considerable positive difference of 25 m is observed. This aligns with our earlier findings in Fig. 12, where a 25 m positioning error is evident at this specific test location when no AP selection schemes are applied. Hence, it can be inferred that the proposed AP selection strategies are successful in bringing the positioning error of the test point down to 0 m.

While the AP selection schemes demonstrates effectiveness in enhancing the localization performance for test points situated at the second floor, it is noticed that the performance improvements for the first and ground floor are not as pronounced. For instance, the test points located from coordinate (2, 23, 3.5) to coordinate (2, 33, 3.5) of the first floor show a substantial reduction in positioning error, whereas other test points on the same level do not exhibit a comparable degree of enhancement. As for the ground floor, there is no significant improvement in localization performance at most test spots. This is due to the reason that the initial error is already low on the ground floor and first story, rendering the use of the AP selection techniques less impactful in terms of improvement.

VI. CONCLUSION

In this paper, we tackle the issue of indoor layout change impacting positioning by proposing a novel AP selection framework with three implementation modes, namely the B-APS, F-APS and Z-APS. By leveraging on the periodically updated RSSs measured from selected RPs, the most suitable APs for localization could be determined. Extensive simulations are carried out to evaluate the performance of the proposed AP selection strategy, and results demonstrate that

the proposed scheme offers superior localization performance compared to the baseline technique. Without the use of the proposed AP selection technique, the system fails to locate approximately 15% of the test points within a 7 m radius. However, with the implementation the AP selection scheme, specifically the Z-APS with 9 zones, the percentage of test points predicted beyond 7 m is significantly reduced to only 2.86% by utilizing only around 10% of the RPs to regularly collect RSS. Besides that, both the F-APS and B-APS also outperform the baseline technique without AP selection, resulting in reduction in average positioning error by 28.86% and 33.53%, respectively. Additionally, a thorough analysis of the effects of P and γ, which are the important parameters of the proposed AP selection scheme, towards the localization accuracy has also been provided. Our investigation suggests that using as low as 0.78% of RPs for regular RSS collection can significantly enhance the localization performance and the range of suitable γ is approximately 22.5 dBm – 25 dBm for Z-APS strategies and 25 dBm – 30 dBm for F-APS and B-APS. These findings underscore the practicality of our proposed AP selection techniques in real-world scenarios with frequent layout changes, ensuring the resilience of the localization system without the need for frequent fingerprint database updates.

REFERENCES

[1] J. Raper, G. Gartner, H. Karimi, and C. Rizos, "A critical evaluation of location based services and their potential," *J. Location Based Services*, vol. 1, no. 1, pp. 5–45, Mar. 2007, doi: 10.1080/17489720701584069.

[2] W. Zhang, X. Hua, K. Yu, W. Qiu, X. Chang, B. Wu, and X. Chen, "Radius based domain clustering for WiFi indoor positioning," *Sensor Rev.*, vol. 37, no. 1, pp. 54–60, Jan. 2017, doi: 10.1108/sr-06-2016-0102.

[3] L. Cheng, A. Zhao, K. Wang, H. Li, Y. Wang, and R. Chang, "Activity recognition and localization based on UWB indoor positioning system and machine learning," in *Proc. 11th IEEE Annu. Inf. Technol., Electron. Mobile Commun. Conf. (IEMCON)*, Vancouver, BC, Canada, Nov. 2020, pp. 528–533, doi: 10.1109/IEMCON51383.2020.9284937.

[4] L. Bai, F. Ciravegna, R. Bond, and M. Mulvenna, "A low cost indoor positioning system using Bluetooth low energy," *IEEE Access*, vol. 8, pp. 136858–136871, 2020, doi: 10.1109/ACCESS.2020.3012342.

[5] J. Zhen, B. Liu, Y. Wang, and Y. Liu, "An improved method for indoor positioning based on ZigBee technique," *Int. J. Embedded Syst.*, vol. 13, no. 3, p. 292, 2020, doi: 10.1504/ijes.2020.109963.

[6] M. H. Azaddel, M. A. Nourian, K. ShahHosseini, S. A. Junoh, and A. Akbari, "SPOTTER: A novel asynchronous and independent WiFi and BLE fusion method based on particle filter for indoor positioning," *Internet Things*, vol. 24, Dec. 2023, Art. no. 100967, doi: 10.1016/j.iot.2023.100967.

[7] N. Singh, S. Choe, and R. Punmiya, "Machine learning based indoor localization using Wi-Fi RSSI fingerprints: An overview," *IEEE Access*, vol. 9, pp. 127150–127174, 2021, doi: 10.1109/ACCESS.2021.3111083.

[8] D. Tse and P. Viswanath, *Fundamentals of Wireless Communication*. Cambridge, U.K.: Cambridge Univ. Press, 2005.

[9] O. Costilla-Reyes and K. Namuduri, "Dynamic Wi-Fi fingerprinting indoor positioning system," in *Proc. Int. Conf. Indoor Positioning Indoor Navigat. (IPIN)*, Busan, South Korea, Oct. 2014, pp. 271–280, doi: 10.1109/IPIN.2014.7275493.

[10] J. Xu, H. Luo, F. Zhao, R. Tao, and Y. Lin, "Dynamic indoor localization techniques based on rssi in WLAN environment," in *Proc. 6th Int. Conf. Pervasive Comput. Appl.*, Port Elizabeth, South Africa, Oct. 2011, pp. 417–421, doi: 10.1109/ICPCA.2011.6106541.

[11] D. Li, Y. Yang, and B. Zhang, "Measurement-based AP deployment mechanism for fingerprint-based indoor location systems," *KSII Trans. Internet Inf. Syst.*, vol. 10, pp. 1611–1629, May 2016, doi: 10.3837/TIIS.2016.04.008.

[12] C. Chen, Y. Chen, Y. Han, H.-Q. Lai, F. Zhang, and K. J. R. Liu, "Achieving centimeter-accuracy indoor localization on WiFi platforms: A multi-antenna approach," *IEEE Internet Things J.*, vol. 4, no. 1, pp. 122–134, Feb. 2017, doi: 10.1109/JIOT.2016.2628713.

[13] B. Dawes and K.-W. Chin, "A comparison of deterministic and probabilistic methods for indoor localization," *J. Syst. Softw.*, vol. 84, no. 3, pp. 442–451, Mar. 2011, doi: 10.1016/j.jss.2010.11.888.

[14] I. Ashraf, S. Din, S. Hur, and Y. Park, "Wi-Fi positioning dataset with multiusers and multidevices considering spatio-temporal variations," *Comput., Mater. Continua*, vol. 70, no. 3, pp. 5213–5232, 2022, doi: 10.32604/cmc.2022.018707.

[15] F. Meneses, A. Moreira, A. Costa, and M. J. Nicolau, "Radio maps for fingerprinting in indoor positioning," in *Geographical and Fingerprinting Data to Create Systems for Indoor Positioning and Indoor/Outdoor Navigation*. New York, NY, USA: Academic, 2019, pp. 69–95. [Online]. Available: http://www.sciencedirect.com/science/article/pii/B9780128131893000046

[16] P. Bahl and V. N. Padmanabhan, "RADAR: An in-building RF-based user location and tracking system," in *Proc. Conf. Comput. Commun., 19th Annu. Joint Conf. IEEE Comput. Commun. Societies*, Tel Aviv, Israel, Mar. 2000, pp. 775–784, doi: 10.1109/INFCOM.2000.832252.

[17] M. Youssef and A. Agrawala, "The Horus WLAN location determination system," in *Proc. 3rd Int. Conf. Mobile Syst., Appl., Services*, Jun. 2005, pp. 205–218, doi: 10.1145/1067170.1067193.

[18] H. W. Khoo, Y. H. Ng, and C. K. Tan, "Enhanced radio map interpolation methods based on dimensionality reduction and clustering," *Electronics*, vol. 11, no. 16, p. 2581, Aug. 2022, doi: 10.3390/electronics11162581.

[19] H. W. Khoo, Y. H. Ng, and C. K. Tan, "A fast and precise indoor positioning system based on deep embedded clustering," in *Proc. Multimedia Univ. Eng. Conf.*, Cyberjaya, Malaysia, Jul. 2022, pp. 38–48.

[20] A. B. Mazlan, Y. H. Ng, and C. K. Tan, "A fast indoor positioning using a knowledge-distilled convolutional neural network (KD-CNN)," *IEEE Access*, vol. 10, pp. 65326–65338, 2022, doi: 10.1109/ACCESS.2022.3183113.

[21] A. B. Mazlan, Y. H. Ng, and C. K. Tan, "Teacher-assistant knowledge distillation based indoor positioning system," *Sustainability*, vol. 14, no. 21, p. 14652, Nov. 2022, doi: 10.3390/su142114652.

[22] F. Potortì et al., "The IPIN 2019 indoor localisation competition—Description and results," *IEEE Access*, vol. 8, pp. 206674–206718, 2020, doi: 10.1109/ACCESS.2020.3037221.

[23] F. Potortì et al., "Off-line evaluation of indoor positioning systems in different scenarios: The experiences from IPIN 2020 competition," *IEEE Sensors J.*, vol. 22, no. 6, pp. 5011–5054, Mar. 2022, doi: 10.1109/JSEN.2021.3083149.

[24] F. Potortì et al., "Offsite evaluation of localization systems: Criteria, systems, and results from IPIN 2021 and 2022 competitions," *IEEE J. Indoor Seamless Positioning Navigat.*, vol. 2, pp. 92–129, 2024, doi: 10.1109/jispin.2024.3355840.

[25] E. Laitinen and E. Lohan, "On the choice of access point selection criterion and other position estimation characteristics for WLAN-based indoor positioning," *Sensors*, vol. 16, no. 5, p. 737, May 2016, doi: 10.3390/s16050737.

[26] H. Miao, Z. Wang, J. Wang, L. Zhang, and L. Zhengfeng, "A novel access point selection strategy for indoor location with Wi-Fi," in *Proc. 26th Chin. Control Decis. Conf. (CCDC)*, Changsha, China, May 2014, pp. 5260–5265, doi: 10.1109/CCDC.2014.6853119.

[27] R. Zhou, Y. Yang, and P. Chen, "An RSS transform—Based WKNN for indoor positioning," *Sensors*, vol. 21, no. 17, p. 5685, Aug. 2021, doi: 10.3390/s21175685.

[28] C. Li, H. Huang, and B. Liao, "An improved fingerprint algorithm with access point selection and reference point selection strategies for indoor positioning," *J. Navigat.*, vol. 73, no. 6, pp. 1182–1201, Nov. 2020, doi: 10.1017/s0373463319000730.

[29] B. Jia, B. Huang, H. Gao, W. Li, and L. Hao, "Selecting critical WiFi APs for indoor localization based on a theoretical error analysis," *IEEE Access*, vol. 7, pp. 36312–36321, 2019, doi: 10.1109/ACCESS.2019.2905372.

[30] P. Huang, H. Zhao, W. Liu, and D. Jiang, "MAPS: Indoor localization algorithm based on multiple AP selection," *Mobile Netw. Appl.*, vol. 26, no. 2, pp. 649–656, Apr. 2021, doi: 10.1007/s11036-019-01411-7.

[31] Y. Xia, Z. Zhang, and L. Ma, "Radio map updated method based on subscriber locations in indoor WLAN localization," *J. Syst. Eng. Electron.*, vol. 26, no. 6, pp. 1202–1209, Dec. 2015, doi: 10.1109/JSEE.2015.00131.

[32] F. Zhao, T. Huang, and D. Wang, "A probabilistic approach for WiFi fingerprint localization in severely dynamic indoor environments," *IEEE Access*, vol. 7, pp. 116348–116357, 2019, doi: 10.1109/ACCESS.2019.2935225.

[33] Y. Tao and L. Zhao, "AIPS: An accurate indoor positioning system with fingerprint map adaptation," *IEEE Internet Things J.*, vol. 9, no. 4, pp. 3062–3073, Feb. 2022, doi: 10.1109/JIOT.2021.3095185.

[34] W. Zhang, K. Yu, W. Wang, and X. Li, "A self-adaptive AP selection algorithm based on multiobjective optimization for indoor WiFi positioning," *IEEE Internet Things J.*, vol. 8, no. 3, pp. 1406–1416, Feb. 2021, doi: 10.1109/JIOT.2020.3011402.

[35] H. Wang, L. Ma, Y. Xu, and Z. Deng, "Dynamic radio map construction for WLAN indoor location," in *Proc. 3rd Int. Conf. Intell. Hum.-Mach. Syst. Cybern.*, vol. 2. Hangzhou, China, Aug. 2011, pp. 162–165, doi: 10.1109/IHMSC.2011.110.

[36] A. N. Nor Hisham, Y. H. Ng, C. K. Tan, and D. Chieng, "Hybrid Wi-Fi and BLE fingerprinting dataset for multi-floor indoor environments with different layouts," *Data*, vol. 7, no. 11, p. 156, Nov. 2022, doi: 10.3390/data7110156.

AQILAH BINTI MAZLAN received the B.Eng. degree (Hons.) in electronics engineering from Multimedia University, Malaysia, in 2022, where she is currently pursuing the master's degree. Her research interests include machine learning and indoor positioning.

YIN HOE NG received the B.Eng. degree (Hons.) in electronics engineering and the Master of Engineering Science and Ph.D. degrees from Multimedia University, in 2004, 2008, and 2013, respectively. He is currently an Associate Professor with the Faculty of Engineering, Multimedia University. Besides that, he is also a Chartered Engineer (C.Eng.) and a Professional Technologist (P.Tech.) registered with Engineering Council United Kingdom and Malaysia Board of Technologists, respectively. His current research interests include advanced signal processing techniques for digital communication systems, machine learning, and indoor positioning.